

University of Massachusetts Boston

ScholarWorks at UMass Boston

Graduate Masters Theses

Doctoral Dissertations and Masters Theses

12-31-2016

A New Class of Integrable Two-Mass Mixtures in One-Dimension

Zaijong Hwang

University of Massachusetts Boston

Follow this and additional works at: https://scholarworks.umb.edu/masters_theses



Part of the [Physics Commons](#)

Recommended Citation

Hwang, Zaijong, "A New Class of Integrable Two-Mass Mixtures in One-Dimension" (2016). *Graduate Masters Theses*. 417.

https://scholarworks.umb.edu/masters_theses/417

This Open Access Thesis is brought to you for free and open access by the Doctoral Dissertations and Masters Theses at ScholarWorks at UMass Boston. It has been accepted for inclusion in Graduate Masters Theses by an authorized administrator of ScholarWorks at UMass Boston. For more information, please contact scholarworks@umb.edu.

A NEW CLASS OF INTEGRABLE TWO-MASS MIXTURES IN ONE-DIMENSION

A Thesis Presented

by

ZAIJONG HWANG

Submitted to the Office of Graduate Studies,
University of Massachusetts Boston,
in partial fulfillment of the requirements for the degree of

MASTER OF SCIENCE

December 2016

Applied Physics Program

©2016 by Zaijong Hwang
All rights reserved

A NEW CLASS OF INTEGRABLE TWO-MASS MIXTURES IN ONE-DIMENSION

A Thesis Presented

by

ZAIJONG HWANG

Approved as to style and content by:

Maxim Olshanii, Professor
Chairperson of Committee

Adolfo del Campo, Associate Professor
Member

Bala Sundaram, Professor
Member

Stephen Arnason, Program Director
Applied Physics Program

Bala Sundaram, Chairperson
Physics Department

ABSTRACT

A NEW CLASS OF INTEGRABLE TWO-MASS MIXTURES IN ONE-DIMENSION

December 2016

Zaijong Hwang, B.S., University of Massachusetts Boston
M.S., University of Massachusetts Boston

Directed by Professor Maxim Olshanii

Among systems with many hard-core point particles that only interact by elastic collisions in one-dimension, it has long been thought that only those with equal mass particles were completely integrable, where the final state of the system through time evolution could be easily predicted from its initial state due to the existence of a maximal number of conserved quantities. In this thesis, we introduce a new class of integrable three-particle systems that contain two unequal masses. These integrable triplets can affect the rate of thermalization in a much larger system composed of particles with two unequal masses, the effect of which is demonstrated with a numerical simulation.

ACKNOWLEDGMENTS

I am indebted to Professors Maxim Olshanii, Stephen Arnason, and Bala Sundaram for their support over my lengthy stay in the master's program. Maxim discovered the integrable system that is the basis for this work, and has long availed to me both his scientific acumen and jovial companionship. Stephen has been guiding my career since I was an undergraduate, doing his best to keep my from wandering off to limbo. Bala has generously provided me with a home on campus, even as I keep taking up more space in his research lab than he uses for himself. This feeble acknowledgment can scarcely express my gratitude. Thank you!

TABLE OF CONTENTS

ACKNOWLEDGMENTS.....	v
LIST OF FIGURES	vii
CHAPTER	Page
1. INTRODUCTION	1
2. GENERALIZED NEWTON’S CRADLES.....	3
2.1 Equal Mass Newton’s Cradles	3
2.2 Unequal Mass Newton’s Cradles	5
3. NUMERICAL SIMULATION OF A TWO-MASS MIXTURE.....	14
4. PARTICLE TRAJECTORIES OVER COLLISION CASCADES	18
5. CONCLUSION AND OUTLOOK	29
CITATIONS	31
LIST OF REFERENCES	33

LIST OF FIGURES

Figure	Page
2.1 Coordinate space of three equal mass particles on an open line	4
2.2 Relative motion of three particles on a line	8
2.3 Determining cascade outcome with method of images	10
3.1 Relaxation time as a function of mass ratio	16
4.1 Heavy-light-heavy triplet trajectories through a cascade of collisions	19

CHAPTER 1

INTRODUCTION

Systems of many hard-core point particles that only interact by elastic collisions in one-dimension are common models for confined cold atoms and classical heat transport. The analysis of such systems is greatly simplified when they are integrable, where the existence of a maximal set of conserved quantities makes it possible to write down relatively simple expressions for the final state of the system in terms of its initial state. Such integrable systems are rare in nature and they can serve as important benchmarks for physical theories and analytical techniques.

In the case of hard-core point particles interacting by elastic collisions in one-dimension, either on an open line or with periodic boundary conditions, the only known integrable model required that all particles be identical and have equal mass [1]. When particles collide with each other under such conditions, they act as if they simply pass through each other, which makes it far easier to predict the behavior of very large number of particles.

This thesis will introduce a new class of integrable hard-core point particles interacting by elastic collisions in one-dimension. These new systems are only integrable with three-particles that possess two unequal masses at specific ratios, must be spatially ordered in a sequence of heavy-light-heavy, and have velocities that will allow the particles to undergo a particular cascade of collisions. This integrability cannot be extended to the

N-body systems that are treatable with equal mass particles. Despite these limitations, the ability to deal with unequal mass particles is nevertheless a significant advancement.

The existence of an integrable triplet with two unequal masses is not merely a mathematical novelty either. Many-body unequal mass systems are fundamentally ergodic [2], making them difficult to treat analytically. The presence of an unequal mass integrable system however, even at the three-particle level, can materially affect the behavior of a much larger system in which the integrable triplets are embedded in. We demonstrate this effect with a numerical simulation of a large mixture of light and heavy particles. The rate at which this large system comes to thermal equilibrium is affected by the mass ratio between the light and heavy particles, and there is a noticeable delay in thermalization when the mass ratio allows locally integrable heavy-light-heavy triplets to arise.

CHAPTER 2

GENERALIZED NEWTON'S CRADLES

Newton's cradle is usually encountered as a simple device used to demonstrate the conservation of energy and momentum. The typical cradle consists of a line of identical pendulums. When a pendulum on one end is lifted and released, it will fall and strike the other stationary pendulums with some velocity. After a cascade of two-body collisions, the pendulum on the other end will be ejected with that same velocity, while all other pendulums are now stationary. There are numerous variations to this basic process, such as imparting multiple pendulums with an initial velocity before the cascade. Although there are many subtleties underlying the operation of the physical Newton's cradle [3], we will overlook these and only focus on one particular phenomenon: if equal mass particles are indistinguishable, then the set of mass-velocity pairs before and after a cascade of collisions should be identical in a Newton's cradle. Taking this as the defining characteristic to preserve for Newton's cradles, we can find a set of generalized Newton's cradles that admit unequal masses while still conserving mass-velocity pairs over a cascade of collisions.

2.1 Equal Mass Newton's Cradles

The task ahead will utilize an obscure coordinate transformation, which we will motivate with an example using a normal equal mass Newton's cradle. Consider for now

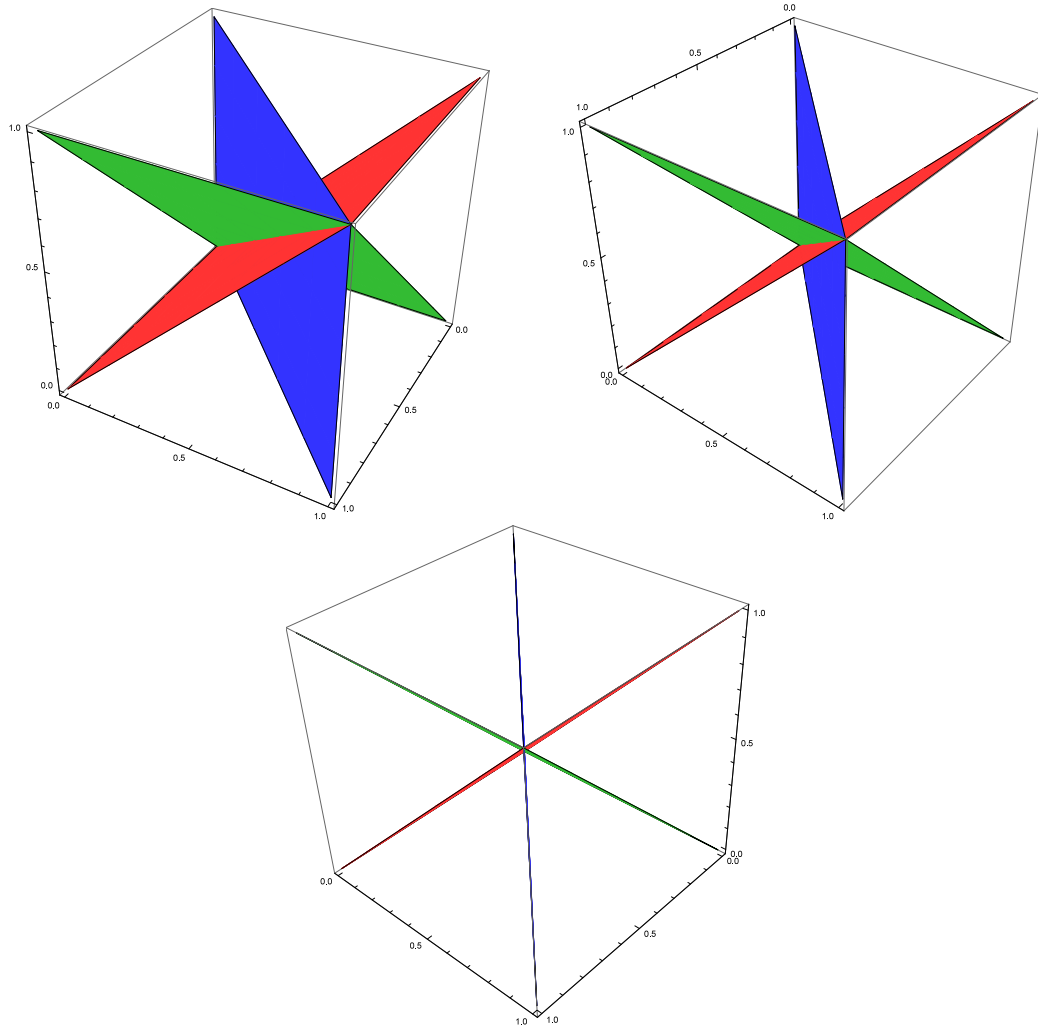


Figure 2.1: Coordinate space of three equal mass particles on an open line. A depiction of the allowed space for particles within the $[0, 1]$ interval is shown in the top left, with a view from the first octant towards the origin in the back corner. The blue, red, and green planes correspond to the contact planes where $x_1 = x_2$, $x_2 = x_3$, and $x_1 = x_3$ respectively. The two other images are identical except their view is rotated towards the line connecting the origin to $(1, 1, 1)$. A two-dimensional view of the system along this line essentially projects the space onto a plane representing the relative motion of the particles and eliminates the center of mass motion. This plane will be partitioned by three contact lines through the origin. The angle between these contact lines will shift if the masses were made unequal, and is what leads to the system seen in Fig. 2.2.

a system of three equal mass hard-core particles on an open line, and let the three particle positions be x_1, x_2, x_3 . This system of three equal mass particles on a line with distinct positions can be represented as a single particle in a three-dimensional space using x_1, x_2, x_3 as the new coordinates. The resulting transformation is depicted in Fig. 2.1, which also shows the contact planes between the particles. In this coordinate space, the motion of a point at any location along the $x_1 = x_2 = x_3$ direction corresponds to the center of mass motion of the original three equal mass particles on the open line. By rotating our viewpoint to align with this direction, we can effectively eliminate the motion of the center of mass.

The final two-dimensional view of the system encodes only the relative motion of the original three equal mass particles on the open line. The two-dimensional plane is naturally partitioned into six sectors, separated by three contact lines through the origin that are the remnants of the three contact planes in the initial three-dimensional coordinate space. The advantage of using this final two-dimensional view is that the evolution of the system from any initial condition will simply trace out a straight line segment between two points on the plane. The intersection between this straight trajectory and the contact lines then represent collisions between the physical particles. Whenever such a trajectory is able to intersect all three contact lines, it will have undergone a cascade of three two-body collisions, and will have the same set of mass-velocity pairs in its final and initial state.

2.2 Unequal Mass Newton's Cradles

The analysis of the equal mass Newton's cradle can be extended to include unequal mass particles by an appropriate rescaling of the x_1, x_2, x_3 coordinates. Such a rescaling

changes the angle between the contact lines in the final two-dimensional view in order to preserve the representation of the time evolution of the system as a straight line trajectory.

Let us now formally consider a system of three hard-core particles on an open line with arbitrary masses m_1, m_2, m_3 and positions x_1, x_2, x_3 . The Lagrangian of this system may be written as

$$L = \frac{1}{2} \sum_{i=1}^3 m_i \dot{x}_i^2 - V(x_1, x_2, x_3). \quad (2.1)$$

Without loss of generality, we may choose $x_1 \leq x_2 \leq x_3$, which will fix the potential as

$$V(x_1, x_2, x_3) = \begin{cases} 0 & \text{if } x_1 \leq x_2 \leq x_3 \\ \infty & \text{otherwise} \end{cases}. \quad (2.2)$$

Using a set of coordinates that produces a scalar mass for the kinetic energy of the relative motion of three particles [4, 5]

$$x = \sqrt{\frac{m_1 m_2}{m_1 + m_2}} (x_1 - x_2), \quad (2.3)$$

$$y = \sqrt{\frac{m_3 (m_1 + m_2)}{m_1 + m_2 + m_3}} \left(\frac{m_1 x_1 + m_2 x_2}{m_1 + m_2} - x_3 \right), \quad (2.4)$$

$$z = \frac{1}{\sqrt{m_1 + m_2 + m_3}} (m_1 x_1 + m_2 x_2 + m_3 x_3), \quad (2.5)$$

the Lagrangian can be transformed into

$$L = \frac{1}{2} (\dot{x}^2 + \dot{y}^2 + \dot{z}^2) + V(x, y, z), \quad (2.6)$$

with a potential of

$$V(x, y, z) = \begin{cases} 0 & \text{if } x \leq 0 \text{ and } y \leq \left(\frac{m_1 m_3}{m_2 (m_1 + m_2 + m_3)} \right)^{\frac{1}{2}} x \\ \infty & \text{otherwise} \end{cases} . \quad (2.7)$$

This coordinate transformation is the same rotation and projection used to treat the equal mass Newton's cradle, where the z direction corresponds to the motion of the center of mass, and some additional factors to account for the unequal masses. These new coordinates are very similar to the standard Jacobi coordinates that are frequently used in solving many-body problems, but the prefactors are substantially different here. The transformation above will always produce a scalar mass, whereas Jacobi coordinates can only guarantee a diagonal mass matrix. The importance of this distinction will become evident shortly.

The new z coordinate is proportional to the center of mass coordinate of the three particles. Since the time evolution of the center of mass is decoupled from the collision dynamics of the particles, we may eliminate the z coordinate from our analysis. The motion of three particles in one dimension can thus be mapped into the motion of one particle of unit mass in two dimensions as seen in Fig. 2.2.

On this two-dimensional plane, the relative positions of the three particles are encoded within the x and y coordinates. The trajectory of the three particles is represented by a ray, the orientation of which determines the relative velocities of the three particles up to a rescaling of time. As a consequence of choosing $x_1 \leq x_2 \leq x_3$, the single point that now represents the relative motion of three particles will be constrained to move within a wedged region bounded by two hard walls.

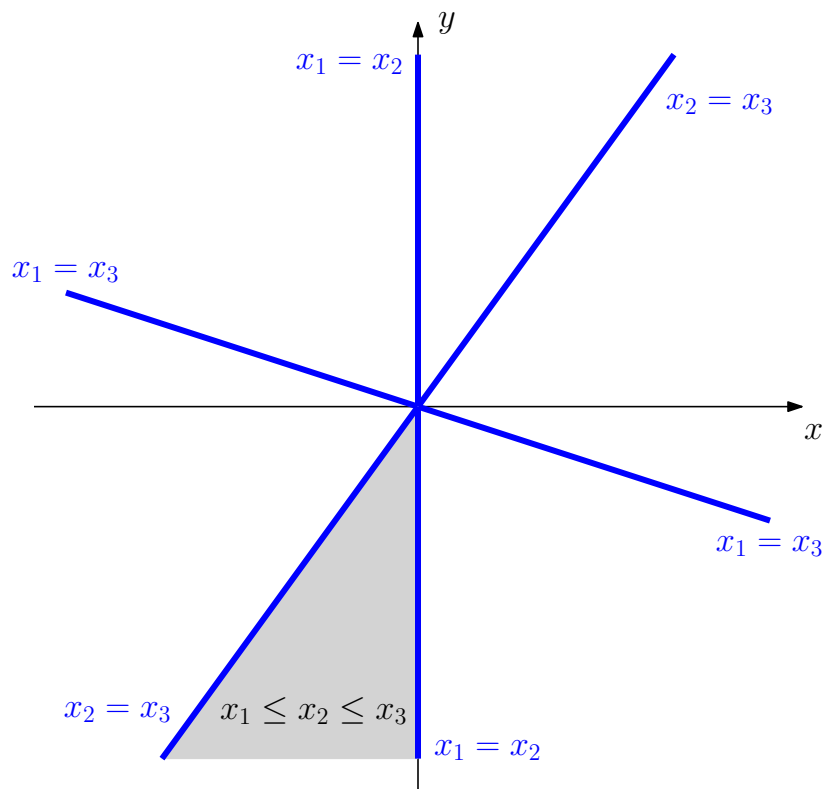


Figure 2.2: Relative motion of three particles on a line. The x and y transformed coordinates above correspond to the the relative motion of three particles on a line. The system is confined to the $x_1 \leq x_2 \leq x_3$ shaded domain by choice. There are six wedged regions that correspond to the possible permutations of three particles on a line. In this figure, we have set $m_1 = m_3 = M$ and $m_2 = m$ with $m/M = \sqrt{5} - 2$. The angle between the $x_1 = x_2$ and $x_2 = x_3$ contact line here is $\pi/5$. The view here is essentially the same as that of Fig. 2.1, except the contact lines are at slightly different angles to account for the unequal masses.

The scalar mass of this point now becomes important as specular reflection is guaranteed to occur whenever the point impacts these walls. The overall setup here resembles that of a dynamical billiard, except for the open boundaries. A proper triangular billiard in this two-dimensional plane with closed boundaries would correspond to a system of two particles in one dimension bounded by two hard walls [6–8].

The presence of specular reflection allows our transformed system to be studied with the method of images as in Fig. 2.3. Consider the case where the $x_1 = x_2$ and $x_2 = x_3$ boundaries cross at an angle of $\theta = \pi/n$ where n is an integer. This allows the wedged region in which the system is confined within to tile the x - y plane through reflections across lines of contact between the particles.

This tiling is significant because it ensures that a given set of initial velocities v_1, v_2, v_3 for three particles will always produce a unique set of final velocities v'_1, v'_2, v'_3 regardless of the order of collisions between the particles. In terms of the rays that represent the trajectory of the system, tiling allows a set of parallel incoming rays to remain parallel with each other after they undergo a cascade of reflections, no matter which wall the rays first connect with. This property can be deduced from Fig. 2.3 by tracing the trajectory of the green line in reverse: such a path will reveal the set of reflections that would occur should the incoming ray have connected with the $x_2 = x_3$ boundary first.

There is a rich mathematical background underlying the system depicted in Fig. 2.3, and we shall make a short digression to introduce some relevant concepts. The shaded region in the figure is the fundamental chamber where the physical system actually resides. The two boundaries enclosing the fundamental chamber can be treated as mirrors, and together they form a kaleidoscope. The normal vector of a mirror is called a root vector, and the two root vectors of a kaleidoscope can be used to generate a collection of

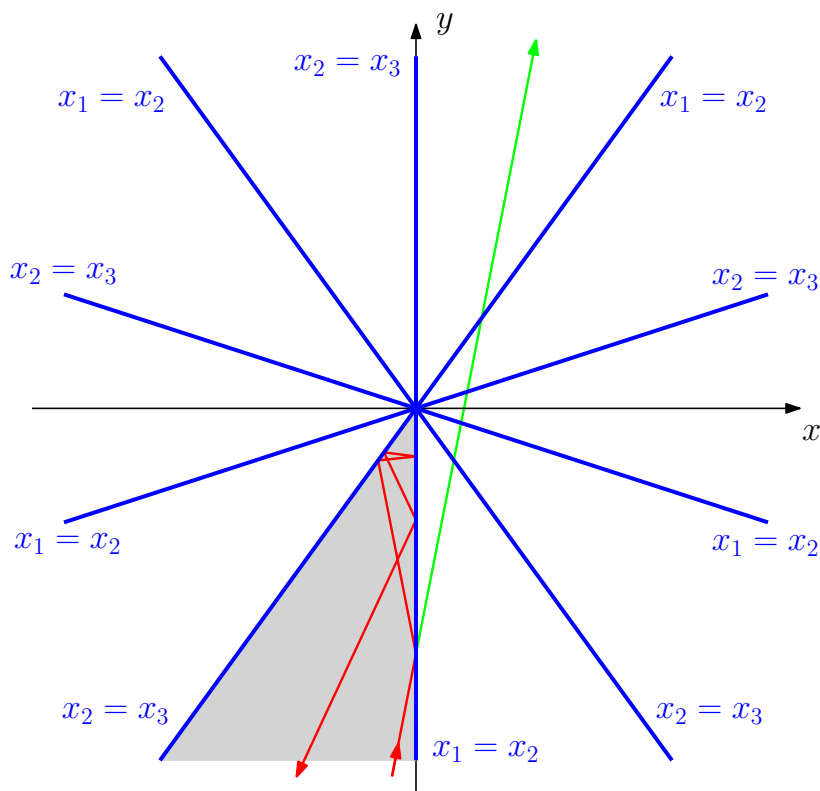


Figure 2.3: Determining cascade outcome with method of images. The time evolution of a system when the light-to-heavy mass ratio is $m/M = \sqrt{5} - 2$ with $\theta = \pi/5$ is shown above. As this corresponds to an odd kaleidoscope, the incoming rays will not in general be parallel to the outgoing rays as in the case of even kaleidoscopes. Shaded region is the $x_1 \leq x_2 \leq x_3$ domain as seen in Fig. 2.2 and now acts as a fundamental chamber of the corresponding reflection group. The actual trajectory of the system as it undergoes specular reflection along the contact lines is shown in red. This trajectory can be obtained from the straight green line by reflecting image chambers repeatedly across contact lines until they overlap with the fundamental chamber.

root vectors that is closed under reflections by the corresponding mirrors. This collection of root vectors forms a root system, which is in turn associated with a reflection group¹. The kaleidoscope in Fig. 2.3 corresponds to the root system $I_2(5)$ and is associated with the dihedral group of the decagon. In general, two-dimensional kaleidoscopes with mirrors at an angle of $\theta = \pi/n$ will correspond to the $I_2(n)$ root systems and be associated with the symmetries of the regular $2n$ -gon [9].

Returning to the two-mass mixture that is the subject of this study, we shall set $m_1 = m_3 = M$ to be the heavy mass and $m_2 = m$ to be the light mass. The mass ratio can then be related to the angle $\theta = \pi/n$ as

$$\frac{m}{M} = \frac{1 - \cos(\pi/n)}{\cos(\pi/n)}. \quad (2.8)$$

If n is odd, a system point which has not experienced any previous collisions will undergo a cascade of n collisions with the walls. The angle between the incoming ray and the first wall will also be equal to that between the outgoing ray and the last wall. In the center of mass frame, this results in the exchange of velocities between the left and right heavy particles while the middle light particle retains its velocity. The mass-velocity pairs will be conserved even if the center of mass velocity is not zero, and such a triplet will therefore constitute a generalized Newton's cradle. The actual outcome of a cascade at

¹We are omitting some details regarding the length of root vectors, which can influence whether the relevant kaleidoscope corresponds to a physical system of particles that are on a line, ring, or confined to an interval.

odd n is

$$\left\{ \begin{array}{c} v_1 \\ v_2 \\ v_3 \end{array} \right\} \xrightarrow[\text{odd cascade}]{n \text{ collisions}} \left\{ \begin{array}{c} v_3 \\ v_2 \\ v_1 \end{array} \right\}. \quad (2.9)$$

Imagine now that three particles with odd n are embedded within a gas of some other particles. Most of the time, this triplet will not manifest the behavior of a Newton's cradle, because the necessary cascade of n two-body collisions are likely to be interrupted by collisions with neighboring particles of the host gas. With finite probability however, the three particles may find themselves in such close proximity that they can complete a cascade of n two-body collisions *uninterrupted*. Given such a complete revival of the local velocity distribution, one would expect a slowdown in the relaxation rate of the many-body system as a whole. This effect will be our focus in the next section.

If n is even, a system point which has not experienced any previous collisions will also undergo a cascade n collisions with the walls, but the incoming and outgoing rays will now remain parallel to each other. In the center of mass frame, this corresponds to a complete reversal of all particle velocities after such a cascade of collisions. The resulting change in velocity distribution is

$$\left\{ \begin{array}{c} v_1 \\ v_2 \\ v_3 \end{array} \right\} \xrightarrow[\text{even cascade}]{n \text{ collisions}} \left\{ \begin{array}{c} V_{CM} - (v_1 - V_{CM}) \\ V_{CM} - (v_2 - V_{CM}) \\ V_{CM} - (v_3 - V_{CM}) \end{array} \right\}, \quad (2.10)$$

where V_{CM} is the center of mass velocity. In principle, such a process is not expected to change the relaxation rate of the many-body system as a whole, although there exist

conditions in which it will come into effect. These circumstances will be relevant in the next chapter as well.

CHAPTER 3

NUMERICAL SIMULATION OF A TWO-MASS MIXTURE

The slowdown in the relaxation rate for a large system due to the presence of heavy-light-heavy triplets that form a generalized Newton's cradle is demonstrated by a numerical simulation with the results shown in Fig. 3.1. The initial condition consists of 100 light and 200 heavy particles randomly positioned within the $[0, 1]$ interval with periodic boundary conditions. We set $M = 1$ and adjust m to achieve different mass ratios. All light particles are initially stationary, while half the heavy particles are randomly chosen to have initial momentum $+1$, and the other half -1 .

In order to determine the rate of thermalization, we need a suitable measure that will place light and heavy particles on an equal footing. The distribution of kinetic energies should then be a good indicator of thermalization due to the eventual equipartition between light and heavy particles. To measure how fast the kinetic energy approaches the Boltzmann distribution, we choose to examine the first non-trivial moment of the kinetic energy distribution, standardized by the mean kinetic energy, as follows

$$\chi \equiv \frac{\langle E_i^2 \rangle}{\langle E_i \rangle^2}, \quad (3.1)$$

where the averages are taken over all $i = 1 \dots 300$ particles. It will have a value of 1.5 under our initial conditions and is expected to rise to 3 if the system is fully thermalized to a Boltzmann distribution. Since equal mass collisions do not contribute to relaxation,

the simulation is carried out over a fixed length of 10,000 light-heavy collisions. At each mass ratio, the simulation is repeated 5,000 times and the average value of χ as a function of the number of light-heavy collisions over these realizations is fit to an exponential curve to extract a time constant.

We choose to use the mean initial frequency of light-heavy collisions as a unit of measurement for the rate of thermalization, because light-heavy collisions are the fundamental interactions that drive thermalization: we expect them to be involved in any universal results that might emerge in the relaxation of a two-mass mixture. One prominent universal result in this vein [10, 11] is that the kinetic energy of hard-core spheres in three dimensions will thermalize across dimensions in 2.7 collisions per particle over a broad range of initial conditions.

Figure 3.1 demonstrates that there are clear peaks in the relaxation time at the expected mass ratios where π/θ is an integer. The background curve also exhibits two expected features. As $m/M \rightarrow 1$ on the right, the relaxation time should diverge as the system is approaching the exactly integrable equal mass configuration. When $m/M \rightarrow 0$ on the left, the relaxation time should also diverge since it will take infinitely many light-heavy collisions to change the velocity of the heavy particles.

Notice that the peaks are present at *both* odd and even values of n . As discussed in the previous section, peaks in relaxation time are expected around odd values of n as a result of local triplets forming a generalized Newton's cradle. For even values of n , a complete uninterrupted cascade of two-body collisions merely reverses all velocities in the center of mass frame, and there is no *a priori* expectation that this will result in a slowdown in the overall rate of relaxation for the many-body system as a whole. Two effects may contribute to these peaks at even n :

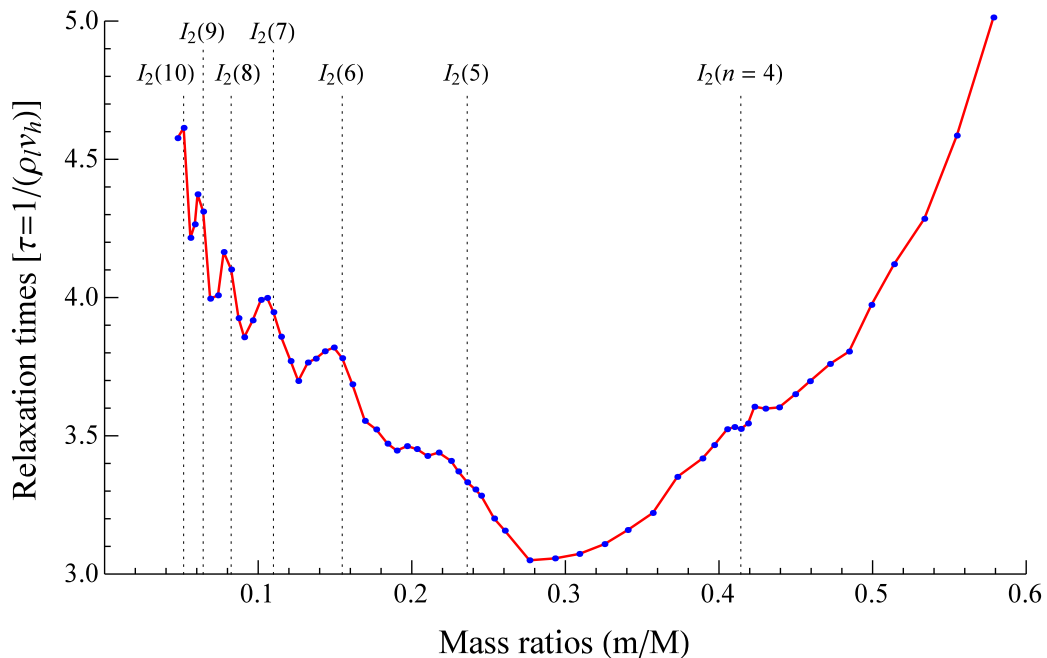


Figure 3.1: Relaxation time as a function of mass ratio. Data points are in blue, and joined by red lines to aid visualization. The vertical axis is the relaxation time $\chi \equiv \langle E_i^2 \rangle / \langle E_i \rangle^2$ (see main text for full definition) in units of $1/(\rho_l v_h)$, where ρ_l is the number density of the light particles, and v_h is the initial speed of the heavy particles. This unit of measurement is an order-of-magnitude estimate for a given heavy particle's initial mean free time between collisions with light particles. Vertical dotted lines correspond to mass ratios where $\theta = \pi/n$ for integer n (see equation 2.8) and peaks are expected to occur. These lines are labeled by the associated $I_2(n)$ root system, starting from $\theta = \pi/10$ on the left and progressing to $\theta = \pi/4$ on the right. The rising background likely contributes to the slight displacement of the peaks from their expected positions.

1. The tiling property for all kaleidoscopes guarantees that any set of initial velocities will always produce a unique set of final velocities after a complete cascade of collisions. The uncertainty in the final velocity distribution is therefore lower at these kaleidoscopic mass ratios when compared to a generic sequence of collisions, for both even and odd n .
2. With our initial velocity distribution, any heavy-light-heavy triplet that is ready to undergo a complete cascade will consist of two heavy particles approaching each other with opposite velocities, and light particle at rest in between them. For this initial condition, the reflection of all velocities about the center of mass velocity after a complete cascade is equivalent to a revival of the initial velocity distribution. As the many-body system continues to relax however, memory of the initial distribution should also erode and weaken this effect.

Neither effects above have been quantified in detail, and a complete explanation for the increase in relaxation time at mass ratios with even n is still required.

CHAPTER 4

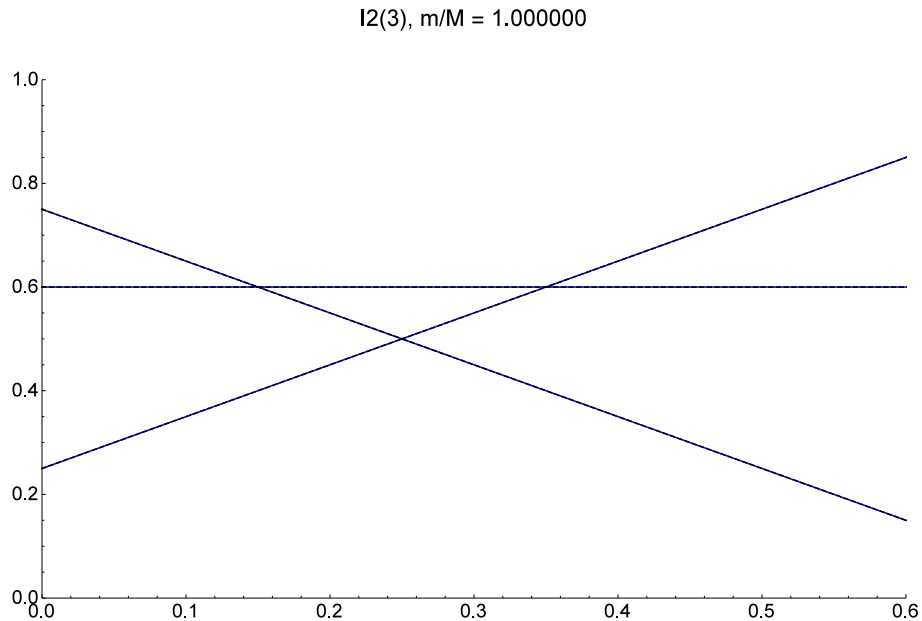
PARTICLE TRAJECTORIES OVER COLLISION CASCADES

The cascade of two-body collisions between three particles that results in the revival of the initial velocity distribution can be elegantly described in terms of the geometry of a set of mirrors forming a kaleidoscope, but it can be difficult to visualize how the underlying particles are actually moving in physical space. Here we will present a series of particle trajectories in physical space that illustrates the dynamics of a heavy-light-heavy triplet of particles undergoing a cascade of collisions in one-dimension.

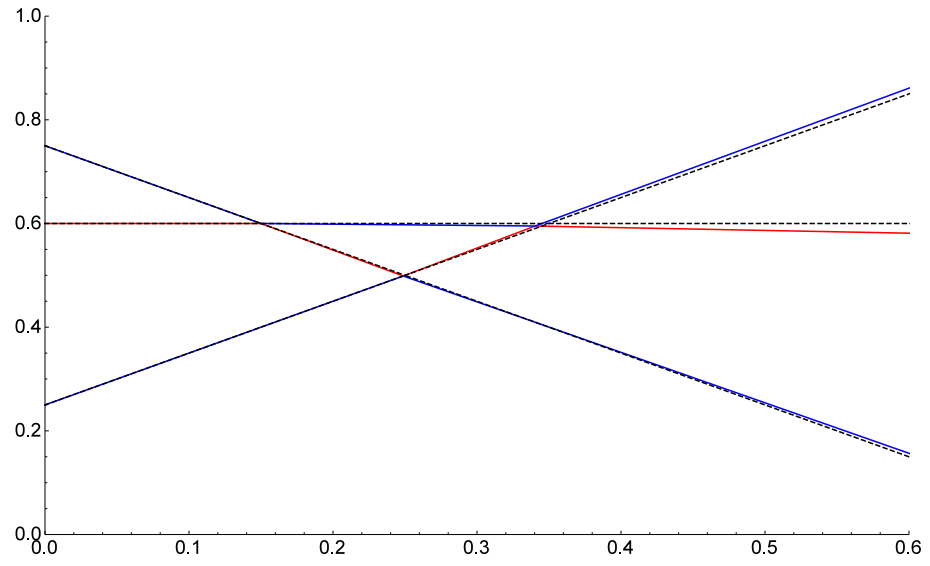
Figure 4.1: Heavy-light-heavy triplet trajectories through a cascade of collisions. The series of graphs below depict the trajectories that result from cascades of two-body collisions between a heavy-light-heavy triplet. Heavy particle trajectories are in blue, while light particle trajectories are in red. All graphs have the same initial condition consisting of a stationary light particle at position 0.6, and two heavy particles moving towards the light particle with a speed of 1, one starting from position 0.3 and the other from position 0.7.

Each graph of position versus time is labeled with the m/M mass ratio of the involved particles. The first graph below consists of three heavy particles of equal masses. This equal mass trajectory is traced out with dashed lines in all ensuing graphs as a reference trajectory.

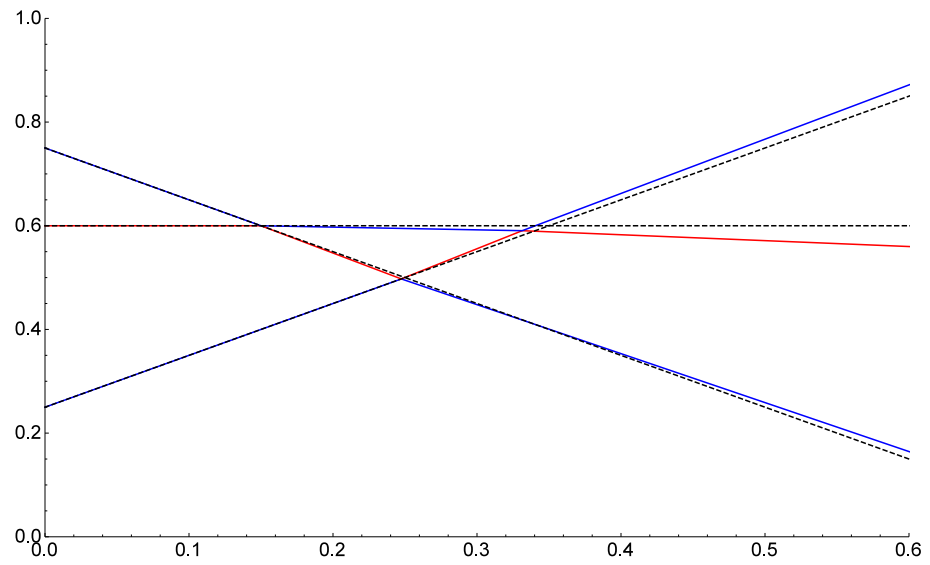
The integrable mass ratios are further marked with the corresponding $I_2(n)$ root system. Notice how the initial velocity distribution is revived after a cascade of n two-body collisions for these mass ratios, and that the cascades all occur within a fixed time interval. The distinction between odd and even mass ratios is also clear here, as odd mass ratio systems will return to follow the equal mass trajectory, whereas even mass ratio systems do not.



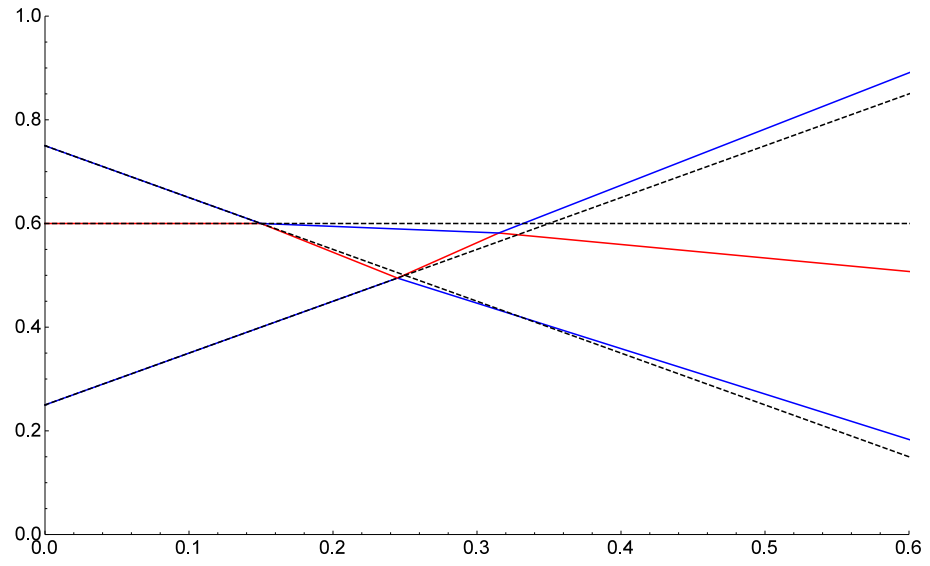
$m/M = 0.950000$



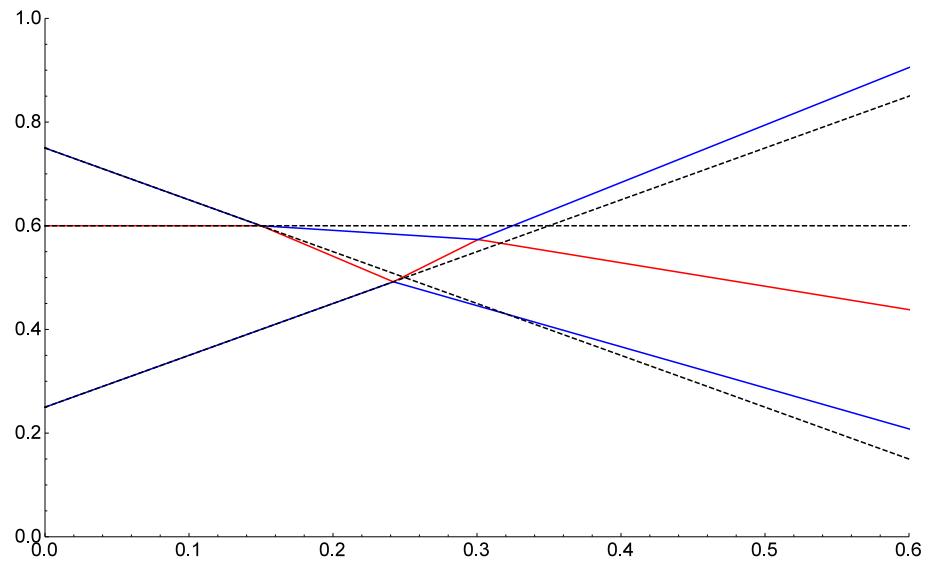
$m/M = 0.900000$



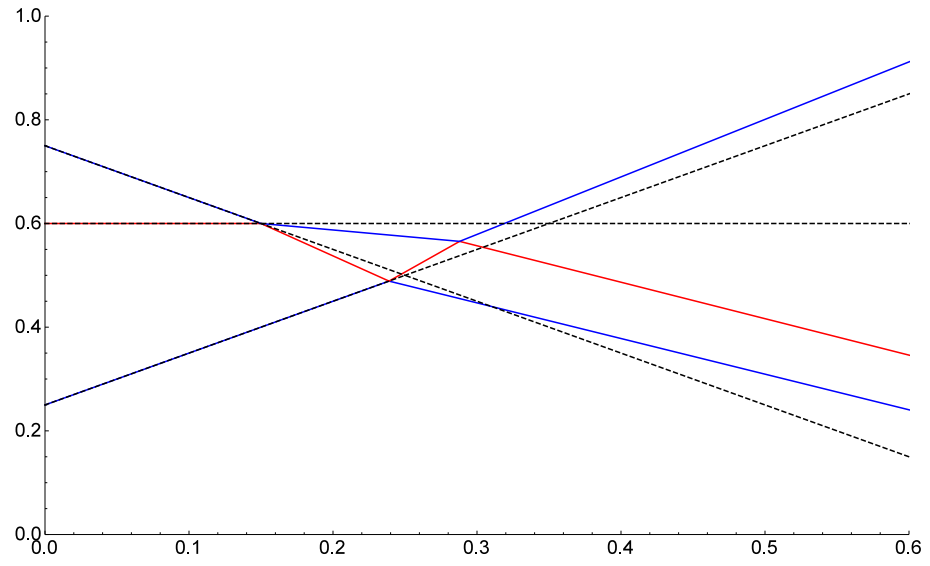
$m/M = 0.800000$



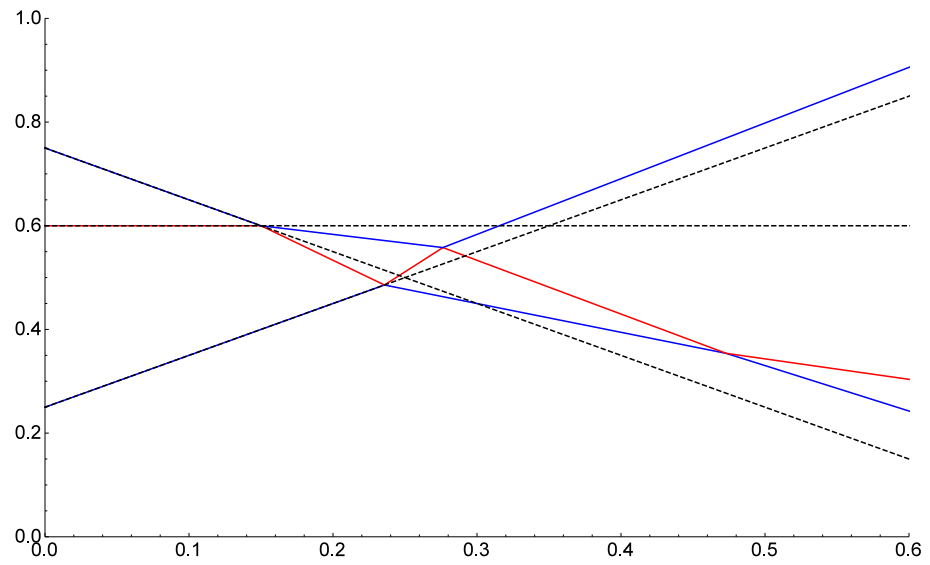
$m/M = 0.700000$



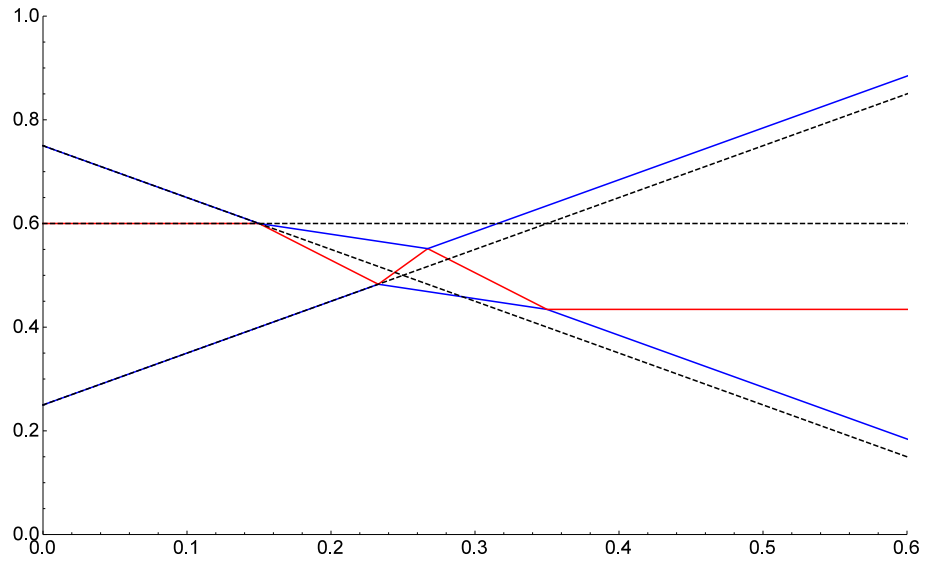
$m/M = 0.600000$



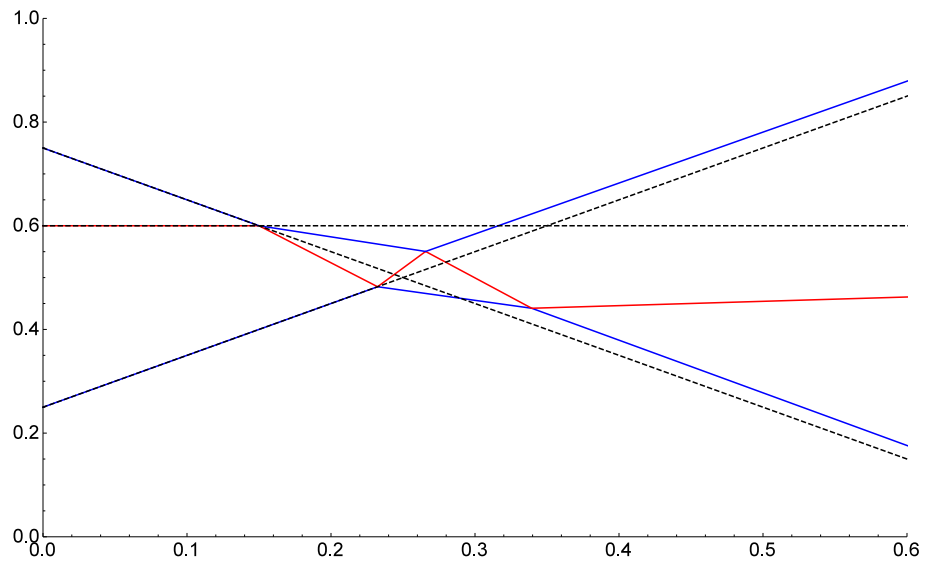
$m/M = 0.500000$



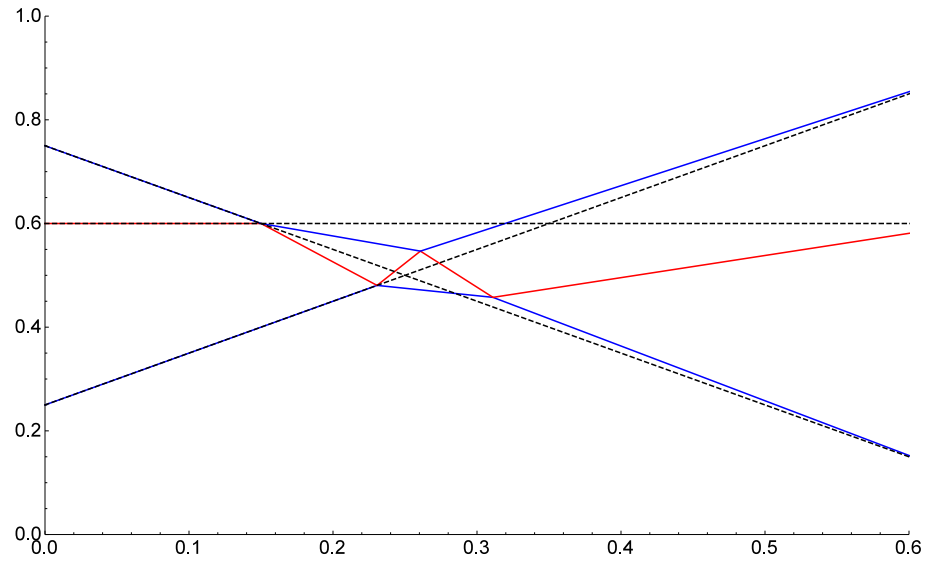
I2(4), m/M = 0.414214



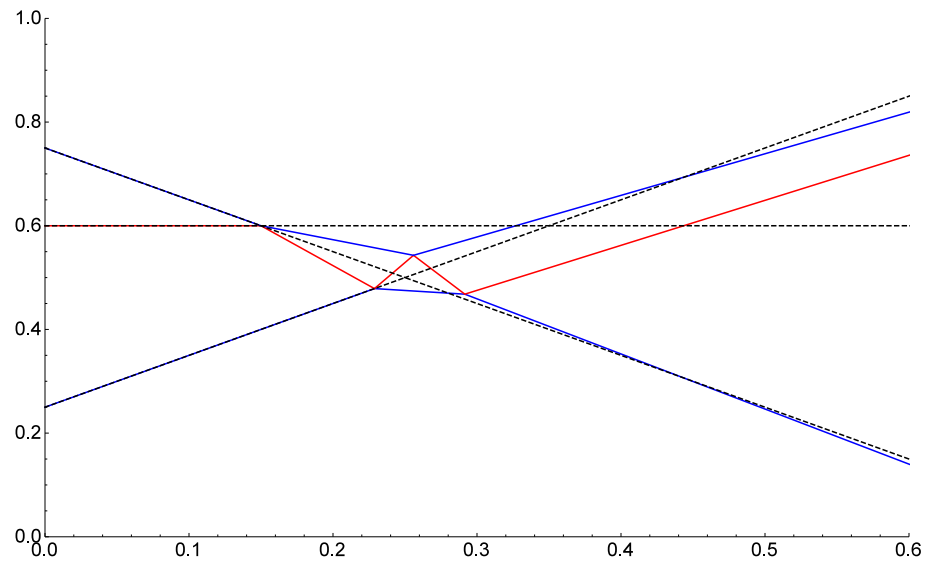
m/M = 0.400000



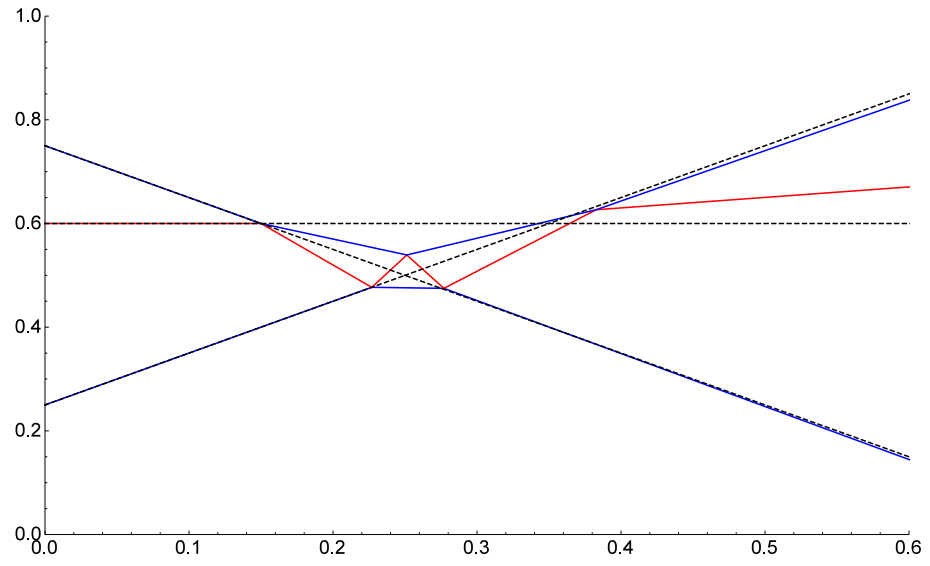
$m/M = 0.350000$



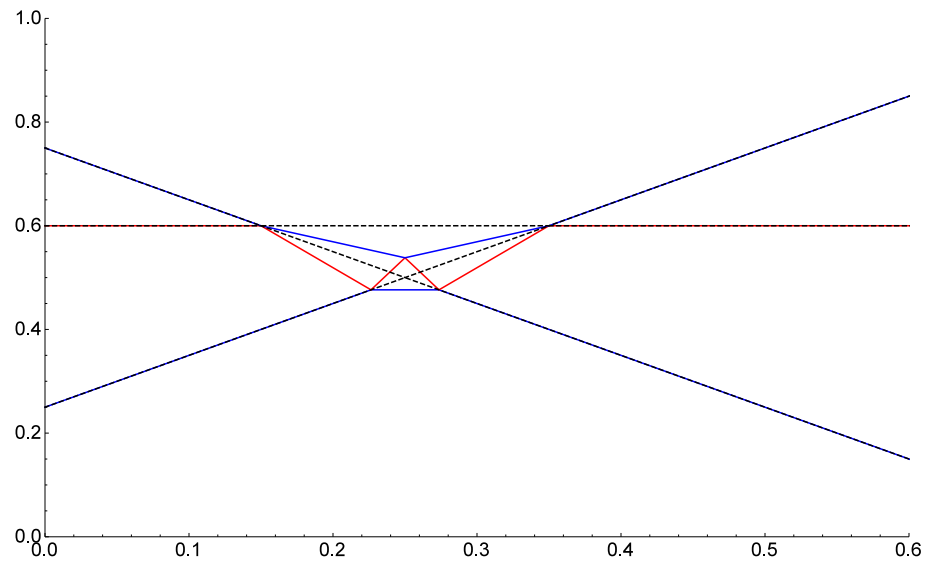
$m/M = 0.300000$



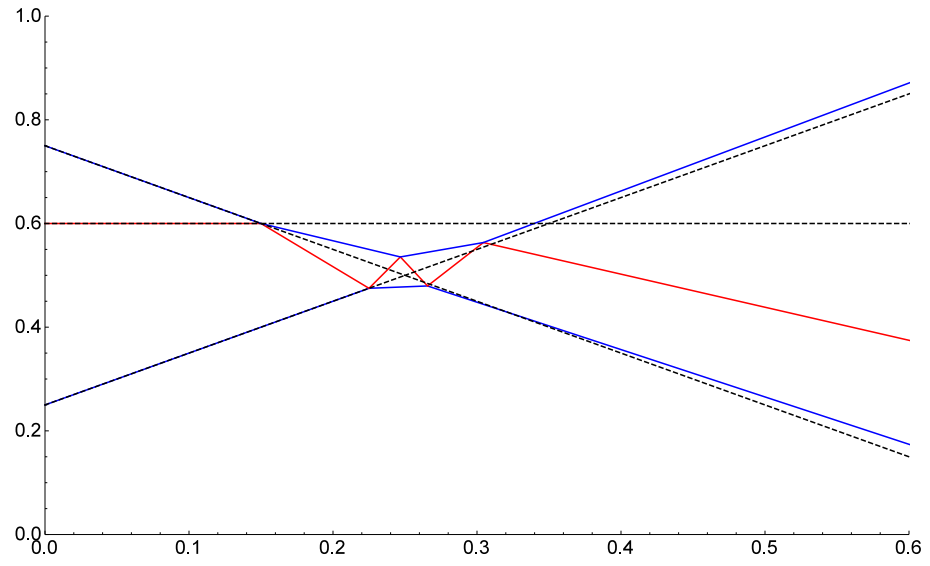
$m/M = 0.250000$



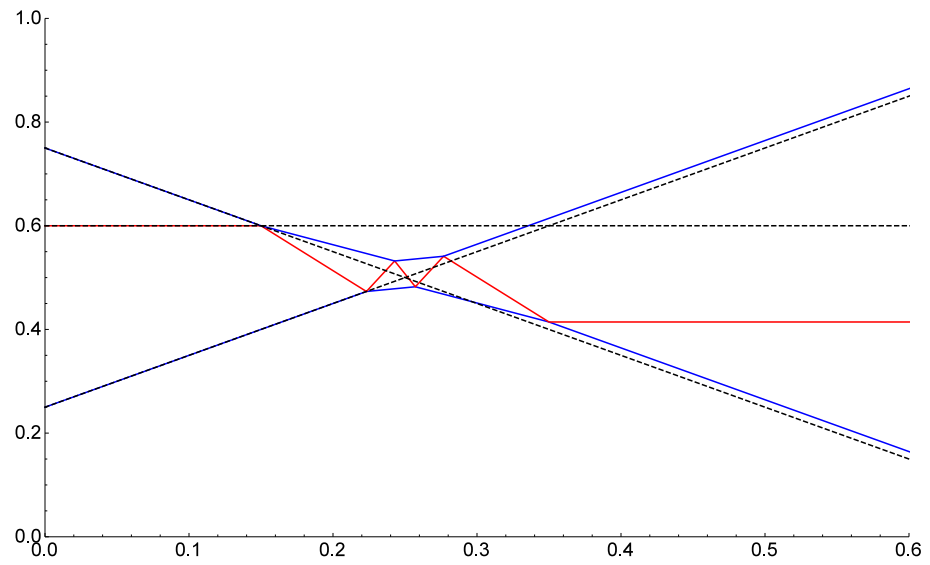
I2(5), $m/M = 0.236068$



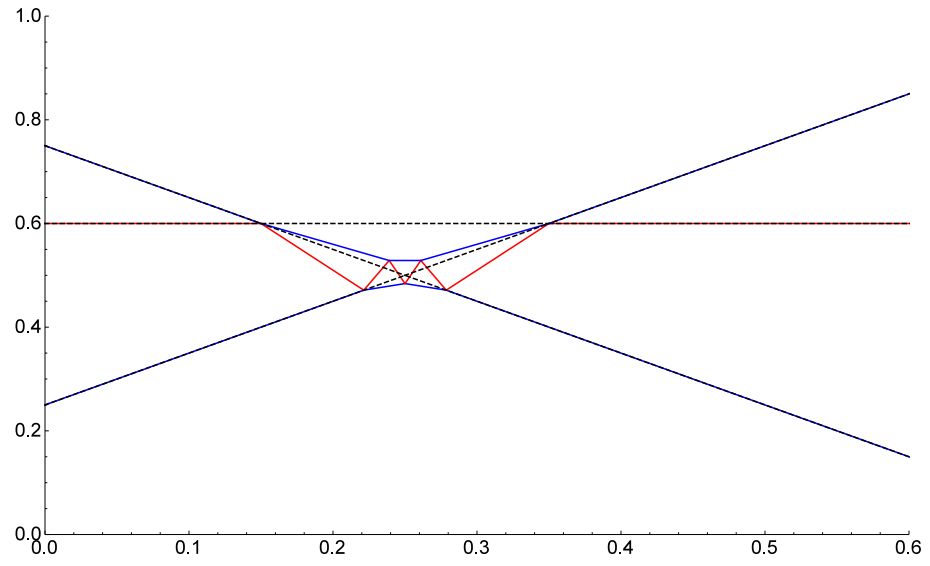
$m/M = 0.200000$



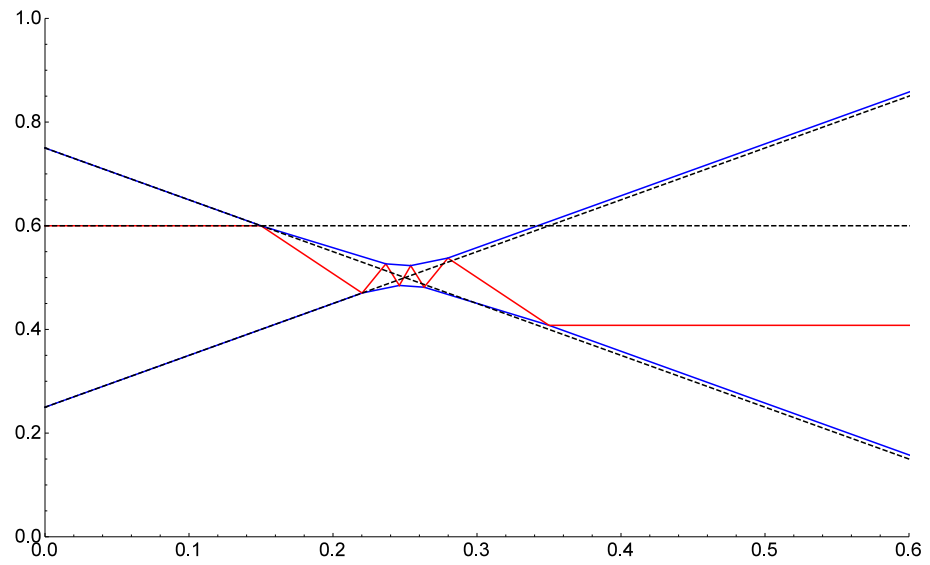
I2(6), $m/M = 0.154701$



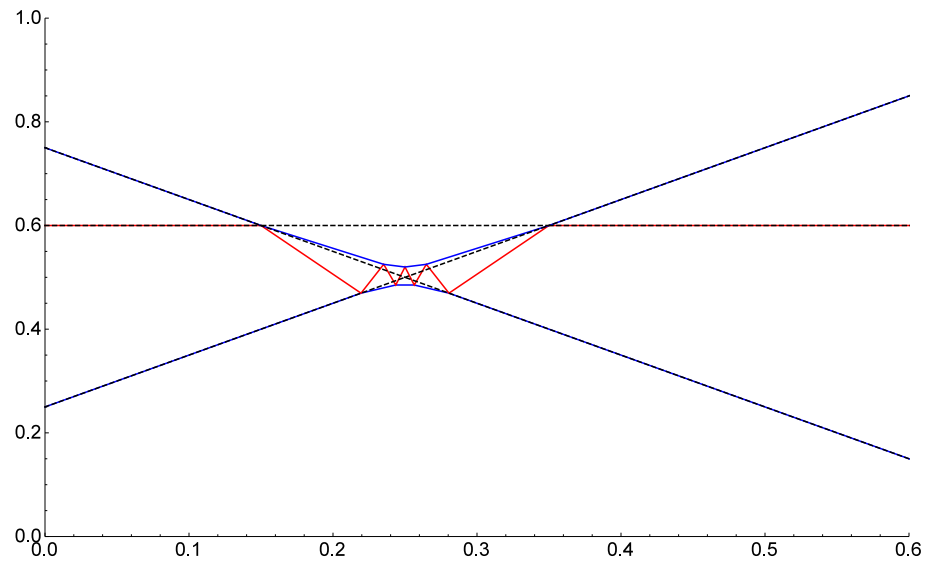
I2(7), m/M = 0.109916



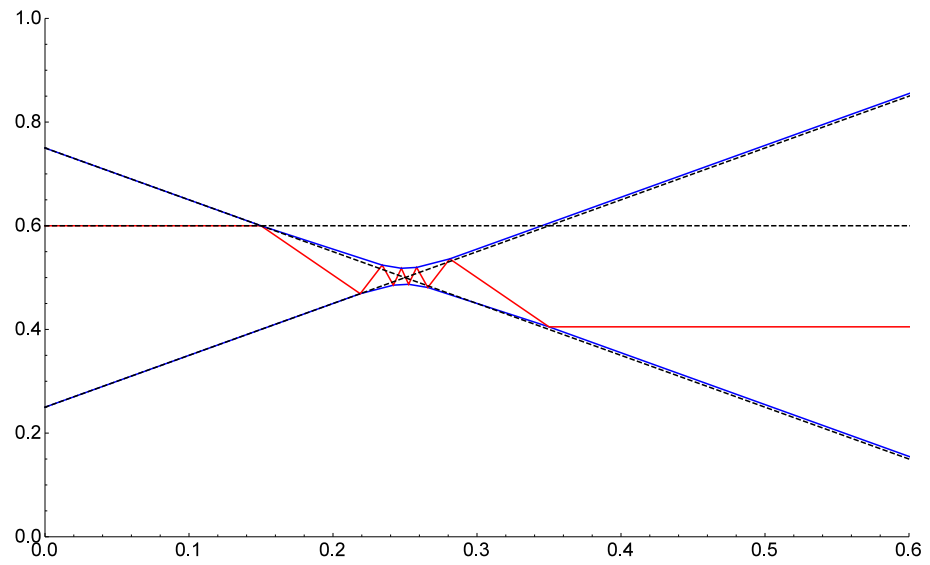
I2(8), m/M = 0.082392



I2(9), m/M = 0.064178



I2(10), m/M = 0.051462



CHAPTER 5

CONCLUSION AND OUTLOOK

Using simple geometric arguments, we showed that a triplet of heavy-light-heavy hard-core particles in one dimension can form a generalized Newton's cradle at particular light-to-heavy mass ratios. This generalized Newton's cradle will preserve the velocity distribution of its constituent particles as they undergo a cascade of collisions: a series of two-body collisions that begins with the triplets not having any prior collisions, and ends with them moving away from each other and never colliding again. We provided numerical evidence that the presence of this generalized Newton's cradle at the three-body level manifests itself in a larger many-body system as peaks in the relaxation time at particular mass ratios.

The expected experimental realization of our model would involve a mixture of two internal states of a single atomic species in an optical lattices, where the ratio between the lattice induced effective masses can be controlled at will. Previous experiments have already produced a mixture of two superfluids of comparable controllable masses [12], and a mixture where one internal state has effectively infinite mass [13].

The present work is a natural continuation of the quest initiated by Michel Gaudin [14, 15] to connect exactly solvable particle problems with kaleidoscopes and root systems. Gaudin originally suggested that only two types of root systems would be relevant to particle problems: A_{N-1} for N equal mass particles on a ring, and C_N for

N equal mass particles between two hard walls on a line. He further demonstrated that any particle problem treatable as a kaleidoscope could be quantized and solved by Bethe Ansatz [14, 16–18].

By considering unequal mass particles, we extend the set of root systems that are relevant to particle problems to include $I_2(n)$ for three unequal mass particles on a line with mass ratios prescribed by equation (2.8). We expect quantized three particle problems with kaleidoscopic mass ratios will also be solvable by Bethe Ansatz. A more general theory for the connection between particle problems and root systems—including an exactly solvable 4-body problem in a box associated with the F_4 root system—will be provided elsewhere [19].

There are several questions that remain open for study. Both the peak-to-background ratio and overall background in Fig. 3.1 require a quantitative theoretical foundation. A better explanation for the peaks in relaxation time at even n is also needed. An interesting possibility for future research is to further extend the set of exactly solvable particle problems by linking previously unexplored root systems to novel particle problems, including those with unequal masses [19].

CITATIONS

- [1] L. Tonks *Phys. Rev.*, vol. 50, p. 955, 1936.
- [2] P. I. Hurtado and S. Redner, “Simplest piston problem. i. elastic collisions,” *Phys. Rev. E*, vol. 73, p. 016136, Jan 2006.
- [3] F. Herrmann and P. Schmälzle, “Simple explanation of a well-known collision experiment,” *Am. J. Phys.*, vol. 49, no. 8, pp. 761–764, 1981.
- [4] D. W. Jepsen and J. O. Hirschfelder, “Set of co-ordinate systems which diagonalize the kinetic energy of relative motion,” *Proc. Natl. Acad. Sci. U.S.A.*, vol. 45, pp. 249–256, 1959.
- [5] J. B. McGuire, “Study of exactly soluble one-dimensional n-body problems,” *J. Math. Phys.*, vol. 5, pp. 622–636, May 1964.
- [6] S. L. Glashow and L. Mittag, “Three rods on a ring and the triangular billiard,” *J. Stat. Phys.*, vol. 87, pp. 937–941, May 1997.
- [7] R. Artuso, G. Casati, and I. Guarneri, “Numerical study on ergodic properties of triangular billiards,” *Phys. Rev. E*, vol. 55, p. 6384, June 1997.
- [8] J. Wang, G. Casati, and T. Prosen, “Nonergodicity and localization of invariant measure for two colliding masses,” *Phys. Rev. E.*, vol. 89, p. 042918, 2014.
- [9] H. S. M. Coxeter, *Regular Polytopes*. London: Methuen & CO. LTD., 1948.
- [10] C. R. Monroe, E. A. Cornell, C. A. Sackett, C. J. Myatt, and C. E. Wieman, “Measurement of cs-cs elastic scattering at $t=30 \mu\text{k}$,” *Phys. Rev. Lett.*, vol. 70, p. 414, 1993.
- [11] H. Wu and C. J. Foot, “Direct simulation of evaporative cooling,” *J. Phys. B*, vol. 29, pp. L321–L328, 1996.
- [12] B. Gadway, D. Pertot, R. Reimann, and D. Schneble, “Superfluidity of interacting bosonic mixtures in optical lattices,” *Phys. Rev. Lett*, vol. 105, p. 045303, Jul 2010.
- [13] B. Gadway, D. Pertot, J. Reeves, M. Vogt, and D. Schneble, “Glassy behavior in a binary atomic mixture,” *Phys. Rev. Lett*, vol. 107, p. 145306, Sep 2011.
- [14] M. Gaudin, *The Bethe Wavefunction*. Cambridge University Press, translated ed., 2014.

- [15] M. Gaudin, "Boundary energy of a bose gas in one dimension," *Phys. Rev.*, vol. A24, p. 386, 1971.
- [16] E. Emsiz, E. M. Opdam, and J. V. Stokman, "Periodic integrable systems with delta-potentials," *Comm. Math. Phys.*, vol. 264, p. 191, 2006.
- [17] E. Emsiz, E. M. Opdam, and J. V. Stokman, "Trigonometric cherednik algebra at critical level and quantum many-body problems," *Sel. math., New ser.*, vol. 14, p. 571, 2009.
- [18] E. Emsiz, "Completeness of the bethe ansatz on weyl alcoves," *Lett. Math. Phys.*, vol. 91, p. 61, 2010.
- [19] S. G. Jackson and M. Olshanii, "An exactly solvable quantum four-body problem associated with the symmetries of an octacube," *New J. Phys.*, vol. 17, p. 105005, 2015.

LIST OF REFERENCES

- R. Artuso, G. Casati, and I. Guarneri. Numerical study on ergodic properties of triangular billiards. *Phys. Rev. E*, 55(6):6384, June 1997.
- H. S. M. Coxeter. *Regular Polytopes*. Methuen & CO. LTD., London, 1948.
- E. Emsiz. Completeness of the bethe ansatz on weyl alcoves. *Lett. Math. Phys.*, 91:61, 2010.
- E. Emsiz, E. M. Opdam, and J. V. Stokman. Periodic integrable systems with delta-potentials. *Comm. Math. Phys.*, 264:191, 2006.
- E. Emsiz, E. M. Opdam, and J. V. Stokman. Trigonometric cherednik algebra at critical level and quantum many-body problems. *Sel. math., New ser.*, 14:571, 2009.
- B. Gadway, D. Pertot, J. Reeves, M. Vogt, and D. Schneble. Glassy behavior in a binary atomic mixture. *Phys. Rev. Lett*, 107:145306, Sep 2011.
- B. Gadway, D. Pertot, R. Reimann, and D. Schneble. Superfluidity of interacting bosonic mixtures in optical lattices. *Phys. Rev. Lett*, 105:045303, Jul 2010.
- M. Gaudin. Boundary energy of a bose gas in one dimension. *Phys. Rev.*, A24:386, 1971.
- M. Gaudin. *The Bethe Wavefunction*. Cambridge University Press, translated edition, 2014.
- S. L. Glashow and L. Mittag. Three rods on a ring and the triangular billiard. *J. Stat. Phys.*, 87:937–941, May 1997.
- F. Herrmann and P. Schmälzle. Simple explanation of a well-known collision experiment. *Am. J. Phys.*, 49(8):761–764, 1981.
- P. I. Hurtado and S. Redner. Simplest piston problem. i. elastic collisions. *Phys. Rev. E*, 73:016136, Jan 2006.
- S. G. Jackson and M. Olshanii. An exactly solvable quantum four-body problem associated with the symmetries of an octacube. *New J. Phys.*, 17:105005, 2015.
- D. W. Jepsen and J. O. Hirschfelder. Set of co-ordinate systems which diagonalize the kinetic energy of relative motion. *Proc. Natl. Acad. Sci. U.S.A.*, 45:249–256, 1959.

J. B. McGuire. Study of exactly soluble one-dimensional n-body problems. *J. Math. Phys.*, 5(1):622–636, May 1964.

C. R. Monroe, E. A. Cornell, C. A. Sackett, C. J. Myatt, and C. E. Wieman. Measurement of cs-cs elastic scattering at $t=30 \mu\text{k}$. *Phys. Rev. Lett.*, 70:414, 1993.

L. Tonks. *Phys. Rev.*, 50:955, 1936.

J. Wang, G. Casati, and T. Prosen. Nonergodicity and localization of invariant measure for two colliding masses. *Phys. Rev. E.*, 89:042918, 2014.

H. Wu and C. J. Foot. Direct simulation of evaporative cooling. *J. Phys. B*, 29:L321–L328, 1996.